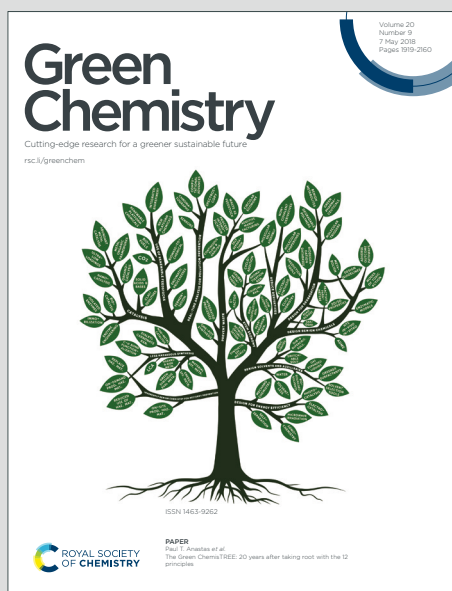


# Green Chemistry

Cutting-edge research for a greener sustainable future

Accepted Manuscript

This article can be cited before page numbers have been issued, to do this please use: L. Peng, M. Wang, H. Li, J. Wang, J. Zhang and L. He, *Green Chem.*, 2020, DOI: 10.1039/D0GC02001J.



This is an Accepted Manuscript, which has been through the Royal Society of Chemistry peer review process and has been accepted for publication.

Accepted Manuscripts are published online shortly after acceptance, before technical editing, formatting and proof reading. Using this free service, authors can make their results available to the community, in citable form, before we publish the edited article. We will replace this Accepted Manuscript with the edited and formatted Advance Article as soon as it is available.

You can find more information about Accepted Manuscripts in the [Information for Authors](#).

Please note that technical editing may introduce minor changes to the text and/or graphics, which may alter content. The journal's standard [Terms & Conditions](#) and the [Ethical guidelines](#) still apply. In no event shall the Royal Society of Chemistry be held responsible for any errors or omissions in this Accepted Manuscript or any consequences arising from the use of any information it contains.

## ARTICLE

## *tert*-Butanol intervention enables chemoselective conversion of xylose to furfuryl alcohol over heteropolyacids

Lincai Peng,\* Mengmeng Wang, Hui Li, Juan Wang, Junhua Zhang and Liang He

Received 00th January 20xx,  
Accepted 00th January 20xx

DOI: 10.1039/x0xx00000x

Both solvent and catalyst play important roles in chemoselective transformation of biomass-related compounds to fine chemicals and fuels. We report here an innovative catalytic strategy for the direct valorization of xylose without external H<sub>2</sub> producing high yield of furfuryl alcohol (FA), a versatile platform molecule. The solvent *tert*-butanol served not only as a precursor of hydrogen honor, but also as a shield to facilitate xylose dehydration and to inhibit polymerization and decomposition reactions of FA. Commercial H<sub>4</sub>SiW<sub>12</sub>O<sub>40</sub> was found to work as a multifunctional catalyst during the cascade conversion, and had a good reusability. The underlying catalytic mechanism revealed that the Brønsted and Lewis acid sites co-existed cooperatively catalyze the xylose dehydration step, and the owned active metal site of W atom adsorbs hydrogen proton to transfer hydrogenation of furfural to FA. After the incorporation of formic acid as a supplemental hydrogen source, an unprecedented FA yield of 90% can be accomplished in a batch reactor under mild conditions. The kinetic behavior describing the conversion of xylose into FA was determined to monitor the process. The estimated activation energies for xylose dehydration, furfural hydrogenation, and FA decomposition were 85.1, 78.8, and 101.1 kJ/mol, respectively. This study opens a new option for the selective production of FA from hemicellulose-derived pentose in a green and straightforward manner.

### Introduction

A sustainable future for the chemical industry eagerly requires efficient strategies to convert biomass-derived carbohydrates into a variety of chemical compounds to displace voluminously consumed petroleum-based building blocks.<sup>1</sup> Xylose, the richest pentose unlocked from a hemicellulose fraction, is a potential feedstock for this purpose because it is mostly present in abundant agroindustrial residues such as sugarcane bagasse, corncob and corn stalk.<sup>2</sup> Xylose-contained lignocellulosic biomass has been industrially utilized to produce furfural (FF) via a stoichiometric mineral acid-catalyzed dehydration reaction.<sup>3</sup> A considerable number of the FF obtained are targeted at furfuryl alcohol (FA) production through partial hydrogenation over copper chromite or other metal-containing catalysts.<sup>4</sup> Current annual production levels are of the order of 200 ktons globally with a staple production capacity in China.<sup>5</sup> The status quo can attribute to the fact that FA is an essential and versatile industrial chemical, supporting its use as an important monomer for synthesizing foundry resins, as well as a precursor for the production of a wide range of green chemicals and fuel additives.<sup>6</sup> Over the past decade, many efforts have been devoted to develop more efficient and eco-friendly catalytic systems in relation to xylose-FF-FA sequential separated reactions.<sup>7</sup> Nevertheless, this multi-step process for FA production exposes energy intensive and costly since

it always involves the pre-production and separation of a chemical intermediate FF.

To overcome these deficiencies, He and co-workers introduced the idea of using a one-pot chemo-enzymatic sequential acid-catalyzed dehydration and bio-reduction process to regulate the conversion.<sup>8</sup> The intermediate separation can be shunned over a specific two-stage arrangement at distinct operating conditions. Alternatively, an integrated chemocatalytic approach to directly transform xylose into FA in a one-pot cascade model is more preferential in terms of sustainability and process economics. The current state-of-the-art processes are summarized in Table S1. Incipiently, Perez and Fraga constructed a dual acid/metal catalytic system composed of sulfated ZrO<sub>2</sub> and Pt/SiO<sub>2</sub> for transforming xylose in a *iso*-propanol/H<sub>2</sub>O mixture, and selectivity towards FA reached *ca.* 50% under a high hydrogen pressure of 30 bar.<sup>9</sup> On this basis, two upgraded studies have been reported from the same group in which single multifunctional catalysts such as Pt/ZrO<sub>2</sub>-SO<sub>4</sub> and Pt/SBA-15-SO<sub>3</sub>H allow the straight formation of FA.<sup>10</sup> Very recently, a noble-metal-free Cu/SBA-15-SO<sub>3</sub>H catalyst had afforded a 62.6% yield of FA directly from xylose in a biphasic *n*-butanol/H<sub>2</sub>O solvent with 40 bar molecular H<sub>2</sub>.<sup>11</sup> On the other hand, a continuous fixed-bed reactor over a combination of H $\beta$  zeolite and Cu/ZnO/Al<sub>2</sub>O<sub>3</sub> using  $\gamma$ -butyrolactone/H<sub>2</sub>O mixture as solvent has also been found to be efficient in the cascade conversion of xylose, giving a 87.2% yield of FA under a 1 bar H<sub>2</sub> feed of 25 mL/min.<sup>12</sup> Despite the positive advances, these strategies suffer from the management of high-pressure external H<sub>2</sub>, using expensive noble-metal or dual catalysts, or low FA yield, which may still turn an economical hurdle for practical application.

BiomassChem Group, Faculty of Chemical Engineering, Kunming University of Science and Technology, Kunming, 650500, China. E-mail: penglincai@kust.edu.cn

† Electronic Supplementary Information (ESI) available: See

DOI: 10.1039/x0xx00000x

Recently, an external H<sub>2</sub>-free process relying on transfer hydrogenation using *iso*-propanol as a hydrogen donor has been proposed to synthesize FA directly from xylose over noble-metal-free catalysts,<sup>13</sup> which opens the opportunity to be more economically feasible facing this cascade reaction. Although a remarkably high selectivity to FA (90–95%) can be achieved over [Al]-SBA-15 molecular sieves, substrate conversion of xylose was less than 15%. Elevated temperature can effectively promote the conversion of xylose, however, the released FA is readily attacked by alcohols to form 2-alkyl furfuryl ether, then ring opening to alkyl levulinate.<sup>14</sup> Formic acid, a major sidestream in biomass processing, is regarded as a promising hydrogen source owing to its high atomic efficiency and excellent stability.<sup>15</sup> Formic acid has been reported as an *in situ* hydrogen supplier for the hydrogenation of FF to FA.<sup>16</sup> Furthermore, the use of formic acid as solvent is beneficial to xylose dehydration process.<sup>17</sup> Nevertheless, it must be pointed out the fact that FA tends to polymerize to yield undesirable solid by-products under acidic environment.<sup>18</sup> Therefore, the controllable and efficient production of FA straight from xylose still remains a key challenge.

In addition to the most investigated catalyst design and optimization of process conditions, solvent effect in selective chemocatalytic conversion of biomass-related compounds to platform molecules has received special attention of late.<sup>19</sup> For instance, xylose processing in  $\gamma$ -valerolactone leads to a significant increase in reaction rate and FF selectivity compared to that in water.<sup>20</sup> Dimethyl sulfoxide (DMSO) stabilizes the positively charged hydroxymethylfurfural (HMF) from liquid-phase reactions of carbohydrates based on the preferential solvation of HMF carbonyl group by DMSO, which reduces its susceptibility to nucleophilic attack and restrains condensation and degradation side-reactions.<sup>21</sup> Formaldehyde pretreatment facilitates lignin monomer production during lignocellulosic biomass fractionation by preventing lignin condensation.<sup>22</sup> In sum, solvent protection strategy expands the options for selective conversion of biomass-derived compounds to fine chemicals.

In this contribution, we for the first time report the chemoselective transformation of xylose to FA over heteropolyacids in *tert*-butanol/formic acid co-solvent system that allows the reaction to proceed in one-pot with an excellent yield and without using external H<sub>2</sub>. Commercially available H<sub>4</sub>SiW<sub>12</sub>O<sub>40</sub> (HSiW) was found to serve as a multifunctional catalyst for xylose dehydration and transfer hydrogenation of FF using formic acid as hydrogen donor. The mechanistic role and importance of the solvent *tert*-butanol towards the selective production of FA were investigated in detail. Also, the kinetic behavior describing the conversion of xylose into FA with this catalytic strategy was explored to monitor the process.

## Results and discussion

### Evaluation of heteropolyacids for xylose processing in *tert*-butanol/formic acid

The preliminary experiment on xylose processing over commercial heteropolyacids using *tert*-butanol as a solvent without external H<sub>2</sub> was performed to evaluate the catalytic behavior. Xylose conversion and the yields of main identified products obtained at 130 °C after 2

h reaction are presented in Fig. 1a (left). It is noted that around 8% xylose was consumed in the absence of a catalyst, both 6-FF and FA cannot be obtained in measurable amounts. The presence of any one heteropolyacid significantly promoted xylose conversion (over 90%), indicating the contribution of acid sites to xylose transformation. More importantly, besides FF that was naturally released from the acid-catalyzed dehydration of xylose, a great deal of FA was produced from FF hydrogenation without the existence of external H<sub>2</sub> over this catalytic system. On the other hand, metal-free acid catalysts (e.g., H<sub>2</sub>SO<sub>4</sub>, Amberlyst-15) were shown to be ineffective for the synthesis of FA from xylose and FF, respectively. When both H<sub>2</sub>SO<sub>4</sub> and metal oxide (e.g., WO<sub>3</sub>, MoO<sub>3</sub>) were used simultaneously, a certain amount of FA can be obtained (see Fig. S1). It is thus conceivable that heteropolyacids act as bifunctional catalysts in the catalytic cascade process. In addition to the acid-catalyzed dehydration of xylose, the active metal sites (e.g., W<sup>6+</sup>, Mo<sup>6+</sup>) in heteropolyacids could catalyze transfer hydrogenation of FF. This claim was further confirmed by using FF as the reaction substrate that the hydrogenation of FF to FA was accomplished over these heteropolyacids (see Fig. 1a (right)).

Nevertheless, previous studies have shown that *tert*-butanol itself did not have hydrogen supply capacity for catalytic transfer hydrogenation reactions.<sup>23</sup> It is worth mentioning that some isobutylene gases were found to be formed during the reaction, which derived from acid-catalyzed intramolecular dehydration of the

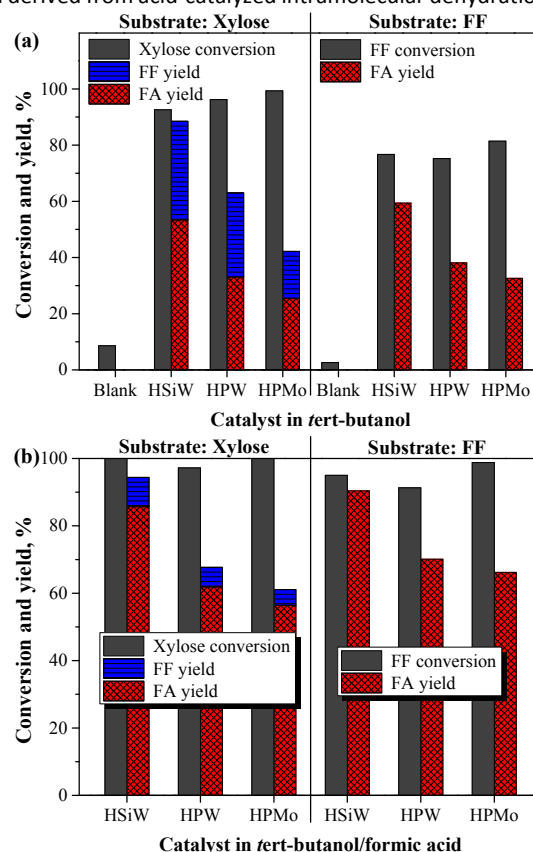


**Fig. 1.** Conversion of xylose and FF to FA over various heteropolyacids in *tert*-butanol (a), and *tert*-butanol/formic acid (b). Reaction conditions: 1 mmol xylose or FF, 0.1 mmol heteropolyacid, 30 mL *tert*-butanol for (a) and 27 mL *tert*-butanol + 3 mL formic acid for (b), 130 °C, 2 h. Abbreviations: HSiW = H<sub>4</sub>SiW<sub>12</sub>O<sub>40</sub>, HPW = H<sub>3</sub>PW<sub>12</sub>O<sub>40</sub>, HPMo = H<sub>3</sub>PMo<sub>12</sub>O<sub>40</sub>.

solvent *tert*-butanol.<sup>24</sup> Moreover, acetone was detected in the product mixture (see Fig. S2). Thus it is reasonably suspected that isobutylene could further oxidized into acetone and formic acid related to the nature of heteropolyacids. As mentioned in some previous reports, formic acid as a hydrogen donor in the transfer hydrogenation process has been well understood for the reduction of carbonyl functionalities.<sup>25</sup> Therefore, we can deduce that the solvent *tert*-butanol may serve as a precursor of hydrogen source to discharge formic acid for transferring hydrogenation of FF to FA in the catalytic action of heteropolyacids.

It is also clear that FF with relatively high yields of 17–35% appeared as a key intermediate from xylose processing in *tert*-butanol over heteropolyacids, suggesting the lack of adequate hydrogen donor to accomplish the transfer hydrogenation of FF. Herein, an external formic acid (it to *tert*-butanol volume ratio of 1:9) was incorporated into reaction system as a supplemental hydrogen donor to convert xylose and FF, and the test results are shown in Fig. 1b. As expected, distinctly improved yields of FA were achieved after the incorporation of formic acid for all tests, and there was a corresponding drop in the amount of FF. Most noticeably of all, the conversion of xylose and FF produced 85.7% and 90.4% yields of FA over HSiW. This suggests that formic acid has superior hydrogen donating capability to realize the transfer hydrogenation of FF to FA under our applied experimental environment. Lately, two studies describing the FF conversion to FA using formic acid as a hydrogen donor were also reported over the catalyst of Rh/ED-KIT-6 and Cu-Pd/C.<sup>16</sup>

Comparing the catalytic behavior of three investigated heteropolyacids, it is observed that HSiW exhibited significantly higher catalytic activity for the selective synthesis of FA in all cases, including the conversion of xylose and FF in *tert*-butanol and *tert*-butanol/formic acid medium, respectively. There was a similar moderate catalytic activity in FA yield between H<sub>3</sub>PW<sub>12</sub>O<sub>4</sub> (HPW) and H<sub>3</sub>PMo<sub>12</sub>O<sub>40</sub> (HPMo) under the identical operating conditions. To illuminate the interrelation of catalyst and its behavior, the used heteropolyacids were characterized with respect to their most fundamental properties for xylose conversion, such as the acidity and the metal reducibility.

NH<sub>3</sub>-TPD profiles from Fig. 2a indicated that one distinct desorption band in the range of 500–600 °C was detected for HSiW and HPW, corresponding to the strong acid strength. The acid amount of HPMo was approximately double that of the foregoing two heteropolyacids, but it was mostly composed of weak acidity. Their individual concentrations of Brønsted and Lewis acid sites were

further quantified by Py-FTIR spectra. As shown in Fig. 2b, Brønsted acid sites occupied the absolute superiority in all tested heteropolyacids as typically described for such materials.<sup>26</sup> On the other hand, compared with HPW and HPMo only having trace Lewis acid sites, HSiW was highlighted in relation to such acid sites. It is known that xylose dehydration is a typical acid-driven reaction, and the catalysts with strong acid strength (e.g., sulfonic acid-functionalized materials) were found to be relatively active in the synthesis of FF in light of extensive reports.<sup>27</sup> Furthermore, the existence of Lewis acid combined with Brønsted acid catalysts have been identified to facilitate xylose transformation into FF through hydride transfer and subsequent dehydration via xylulose as a highly reactive ketose-type intermediate.<sup>28</sup> In our tests, xylulose was indeed detected during the initial stage of the reaction (within 20 min) for HSiW. Therefore, the high total yield towards FF and its derivative FA over HSiW could be attributable to the synergistically contribution of its acid strength, Brønsted and Lewis acidity.

H<sub>2</sub>-TPR test was conducted to evaluate the hydrogen chemisorption capacity of owned metal oxide in the heteropolyacids, and the results are presented in Fig. 2c. HSiW and HPW displayed similar hydrogen chemisorption profiles with one wide reduction peak below 500 °C. The differences are that the peak temperature of HSiW was slightly lower than that of HPW, and the amount of consumed H<sub>2</sub> appeared a little higher. HPMo showed a pair of non-resolved chemisorption peaks above 500 °C, indicating the existence of two reduction stages. It demonstrates that HSiW and HPW have stronger capability of hydrogen chemisorption at low temperature than HPMo. Besides metal site, Lewis acid site has proven to be crucial to hydrogenate the carbonyl group of FF to FA through intermolecular hydride transfer.<sup>29</sup> The cooperation of hydrogen chemisorption capacity and Lewis acidity of HSiW may hold the key to efficiently hydrogenating FF to FA.

Overall, commercial HSiW can be served as a multifunctional and efficient catalyst for the cascade selective conversion of xylose to FA in *tert*-butanol/formic acid co-solvent through dehydration and transfer hydrogenation. The effect of HSiW dosage on xylose processing is given in Fig. S3, and the formation of FA was highly sensitive to HSiW dosage. The reactions were also carried out at elevated substrate concentrations, and a good FA yield of over 65% can still be achieved from 133.3 mmol/L xylose (Fig. S4). When corn-cob-derived xylan was subjected to the reaction instead of xylose, a close chemoselectivity towards FA production was observed with this developed catalytic system (Table S2).

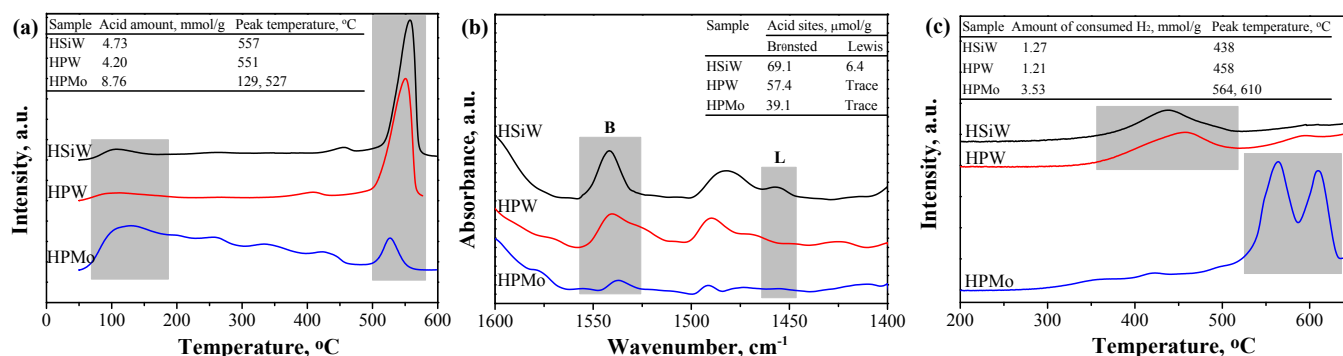
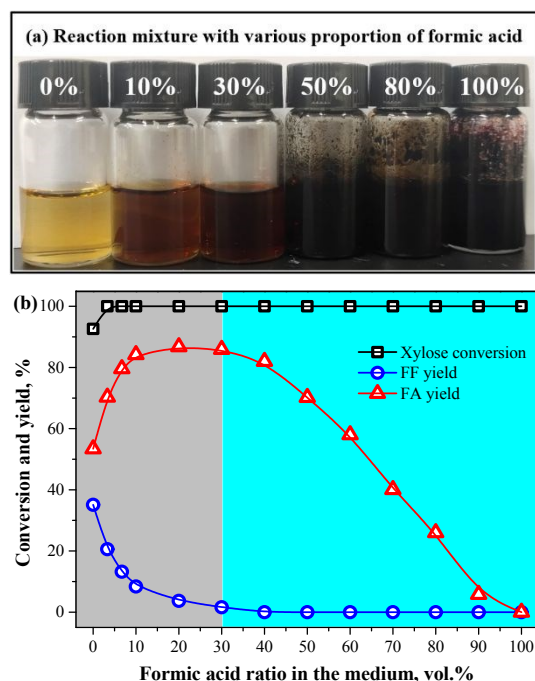


Fig. 2. NH<sub>3</sub>-TPD (a), Py-FTIR (b) and H<sub>2</sub>-TPR (c) results of the HSiW, HPW, and HPMo.

## ARTICLE



**Fig. 3.** Photographs of the reaction mixture with various proportion of formic acid (a), and effect of formic acid dosage on the conversion of xylose in *tert*-butanol-containing medium (b). Reaction conditions: 1 mmol xylose, 0.1 mmol HSiW, the reaction medium consisting of *tert*-butanol and formic acid was fixed at 30 mL, 130 °C, 2 h.

### The role of solvent *tert*-butanol for selective synthesis of FA

Hereinbefore, the solvent *tert*-butanol is just identified as a precursor of hydrogen source, and formic acid is a direct hydrogen donor for transfer hydrogenation of FF. Then whether pure formic acid can be used directly as a solvent for the one-pot conversion of xylose to FA, in the absence of *tert*-butanol. Based on this assumption, the experiments for xylose processing were carried out by incrementing the volume ratio of formic acid to *tert*-butanol. The visualized photograph from Fig. 3a shows that the color of resultant reaction mixture gradually became darker with the increase of formic acid ratio (i.e., the decrease of *tert*-butanol ratio). When the proportion of formic acid exceeded 50%, some dark-brown insoluble solids were produced, portending the occurrence of polymerization secondary reaction. As shown in Fig. 3b, there was an obvious upward trend in FA yield as the formic acid ratio increased from 0 to 10%. Unfortunately, the yield of FA appeared linear and declined rapidly when the formic acid ratio was over 30%, and hardly any FA was detected in pure formic acid. Accordingly, the importance of *tert*-butanol towards the selective production of FA is highly noteworthy. The stability measurement of FA in various solvents displays from Fig. 4 that FA was totally consumed in pure formic acid, obtaining plenty of solid polymers. Clearly, a mere handful of FA

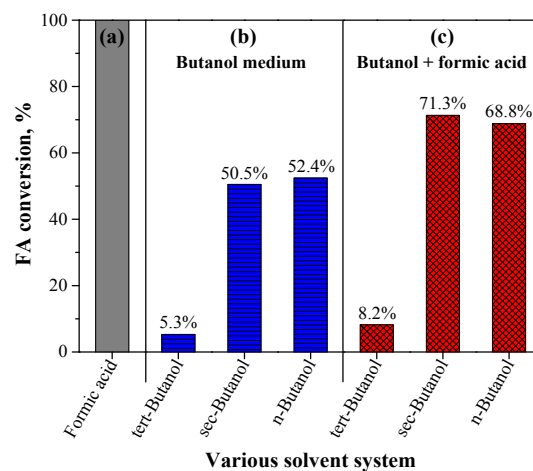


**Fig. 4.** Stability evaluation of FA in pure formic acid (a), various butanol (b), and butanol/formic acid mixture (c). Reaction conditions: 1 mmol FA, 0.1 mmol HSiW, 130 °C, 2 h. 30 mL formic acid for (a), 30 mL butanol for (b), and 27 mL butanol + 3 mL formic acid for (c).

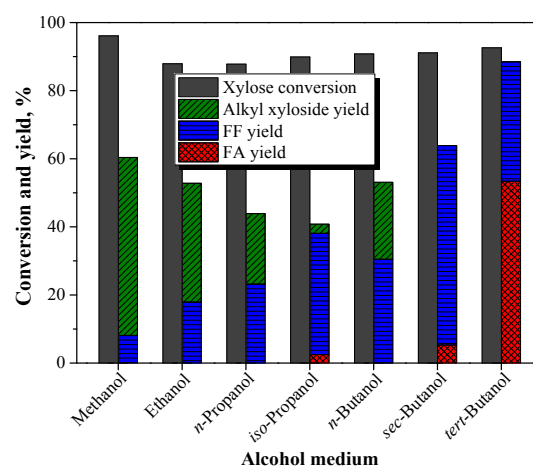


**Fig. 5.** Reactivity of xylose in various alcohol medium. Reaction conditions: 1 mmol xylose, 0.1 mmol HSiW, 30 mL alcohol, 130 °C, 2 h.

were converted in pure *tert*-butanol and *tert*-butanol/formic acid mixture (a volume ratio of 9:1), indicating a good stability in *tert*-butanol-containing medium. However, when other butanols (e.g. *sec*-butanol and *n*-butanol) were used as the solvent instead of *tert*-butanol, a remarkably high FA conversion (50–71%) was observed. 2-Butyl furfuryl ether and butyl levulinate were the main derivatives from FA alcoholysis. The above findings suggest that *tert*-butanol effectively restrains undesirable polymerization and alcoholysis reactions of FA, therefore stabilizing the formed FA. The possible mechanistic role of *tert*-butanol is the preferential solvation of FA by *tert*-butanol protonation if the reaction is performed in a *tert*-butanol-rich mixed solvent, which prevents FA condensation by forming hydrogen bonds with *tert*-butanol to protect its reactive



**Scheme 1.** Mechanistic role of the solvent *tert*-butanol for selective production of FA straight from xylose.

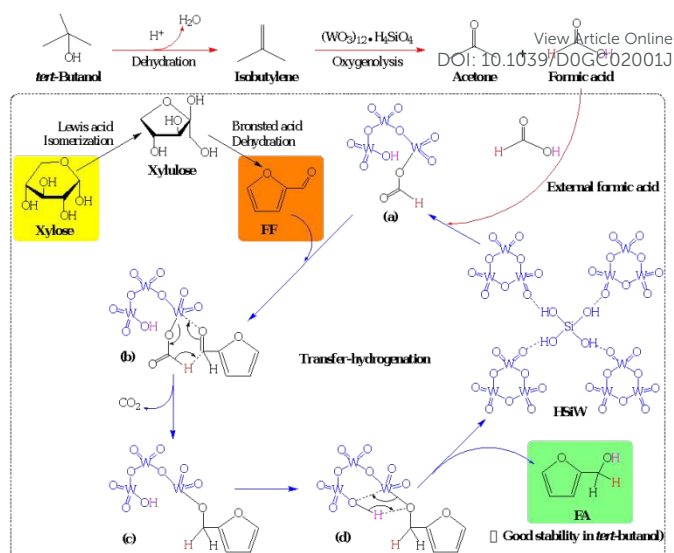
hydroxyl group.<sup>18a,21a</sup> On the other hand, the etherification of FA with *tert*-butanol is torpid due to severe steric effect of *tert*-butanol. Such dual role of *tert*-butanol allows xylose processing to tailor high selectivity towards FA.

Further, various pure alcohols as the reaction medium were explored for the conversion of xylose over HSiW. As shown in Fig. 5, a considerable amount of alkyl xyloside was obtained from the glycosylation of xylose with linear alcohols, which is identified to be harder than xylose for dehydration reaction.<sup>30</sup> Although secondary alcohols (e.g., *iso*-propanol and *sec*-butanol) exhibited good performance in catalytic transfer hydrogenation elsewhere, it displayed poor capability for hydrogenating FF to FA in this work. This could potentially be linked to the catalyst used. On the whole, the total yield of FF and its derivative (FA) was found to raise as increasing the carbon chain length of alcohol from methanol to *n*-butanol, as well as changing alcohols from *n*-butanol to *sec*-butanol and *tert*-butanol. This means the improvement of the extent of xylose dehydration, which may be attributed to increased hydrophobicity and steric effect of alcohol to minimize glycosylation of xylose.

From the above observations, the solvent *tert*-butanol served multiple functions in the selective production of FA straight from xylose, as illustrated in Scheme 1. Firstly, *tert*-butanol worked as a precursor of hydrogen honor to release formic acid for transferring hydrogenation of FF to FA. Then, *tert*-butanol promoted xylose dehydration process based on its strong hydrophobicity and severe steric effect to minimize side reactions. More importantly, *tert*-butanol acted as a stabilization species for the targeted FA, which restrains undesirable polymer-formation and degradation reactions.

### Mechanism of xylose processing in *tert*-butanol/formic acid over HSiW

As exposed hereinbefore, a high selectivity and yield of FA was achieved from nearly 100% xylose conversion in *tert*-butanol/formic acid over HSiW. To more fully understand the chemoselectivity towards product distribution, the carbon balance results for xylose processing with the developed catalytic system are given in Table S3. Other than the front determined FF and FA, a very small amount of *tert*-butyl furfuryl ether (BFE) and solid polymers were produced from the etherification and polymerization of FA, respectively. The total proportion of known products from xylose conversion can be up to 98.6%. Based on all above elaboration covering catalyst



**Scheme 2.** Proposed reaction mechanism for the conversion of xylose to FA in *tert*-butanol/formic acid medium over HSiW.

behavior and solvent effect, as well as qualitative identification compounds, an underlying reaction mechanism of xylose processing in *tert*-butanol/formic acid over HSiW was proposed. As shown in Scheme 2, xylose is first isomerized to xylulose relying on Lewis acid sites of HSiW, which is subsequently dehydrated to FF in the action of Brønsted acid sites.<sup>28</sup> The solvent *tert*-butanol facilitates xylose dehydration process thanks to its stronger hydrophobicity and steric effect to minimize glycosylation of xylose. This is followed by a catalytic cycle involving the transfer hydrogenation of FF to FA using formic acid as the hydrogen donor. Formic acid can be in-situ generated together with acetone from the intramolecular dehydration and oxygenolysis of *tert*-butanol via isobutylene as an intermediate species, as a result of the owned acidic and oxidizing characteristics of HSiW. In the triggered step, formic acid is adsorbed on the W-related site of HSiW surface and dissociated to yield the corresponding W-bound formate species (a). The carbonyl of FF is then coordinated with this formate to form a cyclic six-membered transition state (b). A hydride shift between the formate and the electron-deficient C of FF carbonyl group occurs, giving the intermediate species (c) along with the release of CO<sub>2</sub>. Finally, the hydron on the HSiW is transferred to the electron-rich O of furfuryl alkoxide by the intramolecular concerted process of a transition state species (d), resulting in the formation of FA. The in-situ generated formic acid from *tert*-butanol is the rate-determining step in the transfer hydrogenation of FF to FA, and the external formic acid effectively promotes this transfer hydrogenation process. Coupled with the good stability of FA in *tert*-butanol solvent, the selective production of FA from xylose can be accomplished in a one-pot model of integrating dehydration and hydrogenation reactions.

### Kinetic behavior on the one-pot conversion of xylose to FA

In order to enhance the understanding of xylose conversion in *tert*-butanol/formic acid over HSiW to selectively synthesize FA, the kinetic behavior with different temperatures was studied. The experimental results are shown in Fig. 6a–c. It is known that FF is a key intermediate during this reaction process. A simplified model was applied to study the kinetics of xylose processing, as proposed in

## ARTICLE

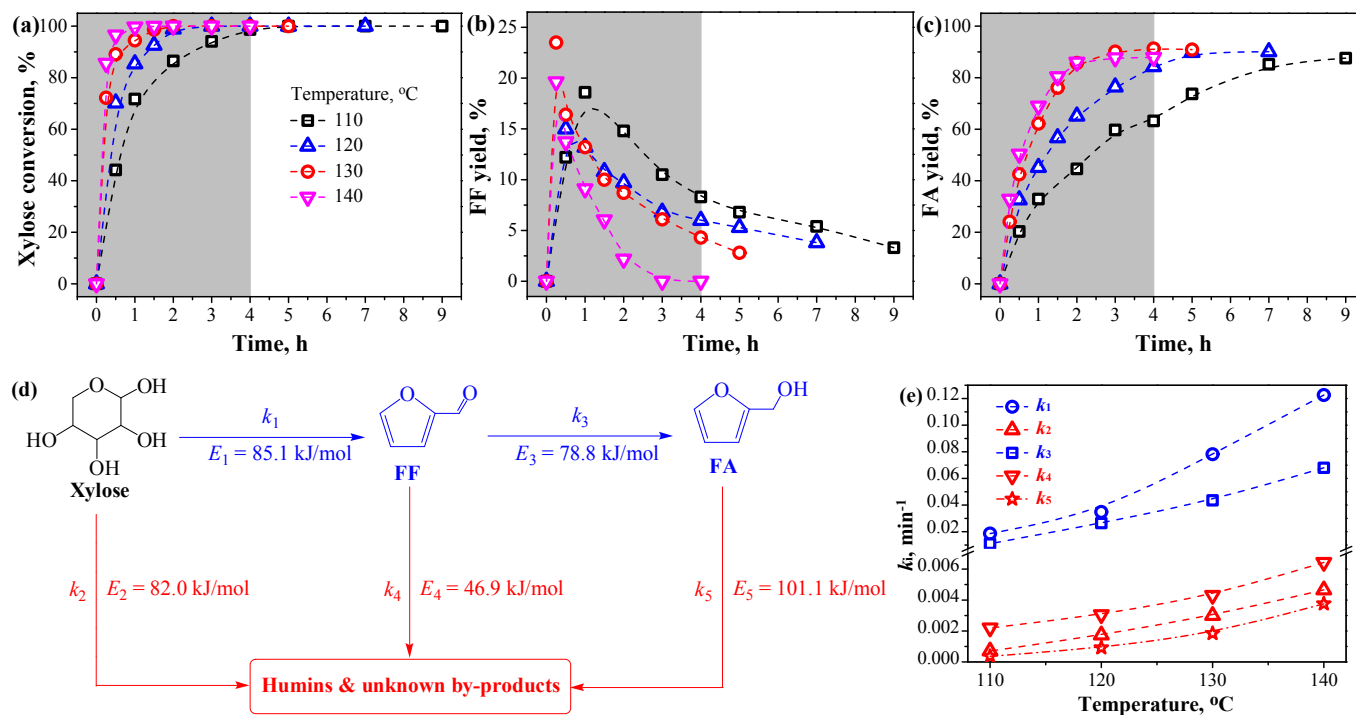


**Fig. 6.** Effect of reaction temperature as a function of time on xylose conversion (a), FF yield (b), and FA yield (c). Reaction conditions: 1 mmol xylose, 0.1 mmol HSiW, 27 mL *tert*-butanol, 3 mL formic acid. Kinetic model for the conversion of xylose to FA in *tert*-butanol/formic acid over HSiW (d). Reaction rate constants of each step under various temperatures (e).

Fig. 6d. The conversion of xylose to FF, FA and side-reactions was assumed to be a pseudo-first-order reaction, which can be expressed by the following equations:

$$\frac{dC_{Xy}}{dt} = -(k_1 + k_2)C_{Xy} \quad (1)$$

$$\frac{dC_{FF}}{dt} = k_1C_{Xy} - (k_3 + k_4)C_{FF} \quad (2)$$

$$\frac{dC_{FA}}{dt} = k_3C_{FF} - k_5C_{FA} \quad (3)$$

Where  $k_i$  ( $i = 1, 2, 3, 4, 5$ ) are the reaction rate constants of each step.  $C_{Xy}$ ,  $C_{FF}$  and  $C_{FA}$  are the concentrations of xylose, FF and FA, respectively.

To derive more reliable kinetic results, the experimental data using FA as the starting substrate in Fig. S5 were first fitted by Equation (S1) to obtain  $k_5$ . Then, Equations (S2) and (S3) were employed to fit the experimental data using FF as the starting substrate in Fig. S6 to obtain  $k_3$  and  $k_4$ . On these basis,  $k_1$  and  $k_2$  were obtained by fitting the experimental data of xylose processing in Fig. 6a–c using Equations (1), (2) and (3). A good correlation ( $R^2 > 0.95$ ) between the measured and predicted values was observed by parity plots (Fig. S7). The reaction rate constants of each step at different temperatures are illustrated in Fig. 6e. The rate constants for xylose dehydration and FF hydrogenation to FA were an order of magnitude larger than those for the decomposition of xylose, FF and FA to by-products,

indicating a highly positive trend towards the production and accumulation of FA.

The Arrhenius law was used to calculate the apparent activation energy (Fig. S8). Interestingly, a significant decrease in activation energy (85.1 kJ/mol) was observed for xylose dehydration in *tert*-butanol/formic acid over HSiW, compared to the known Brønsted acid-catalyzed xylose dehydration in aqueous solution (ca. 130 kJ/mol).<sup>31</sup> However, the activation energy of FF hydrogenation to FA in this investigation (78.8 kJ/mol) was higher than that in the previous reports using high-pressure molecular H<sub>2</sub>.<sup>32</sup> Focusing on the present cascade reaction, it is noted that the activation energies of xylose dehydration and FF hydrogenation were obviously lower than the activation energy of FA decomposition (101.1 kJ/mol). This means that the selectivity of the cascade reaction is dependent on the temperature, and elevated temperature accelerates undesirable reaction of FA decomposition into by-products. Therefore, the selective production of FA from one-pot conversion of xylose can be accomplished by regulating the operating conditions. An excellent FA yield of around 90% was achieved at 130 °C for 3 h or 120 °C for 5 h. The developed kinetics can offer an effective tool to monitor the process and tailor the reaction conditions to obtain the targeted product.

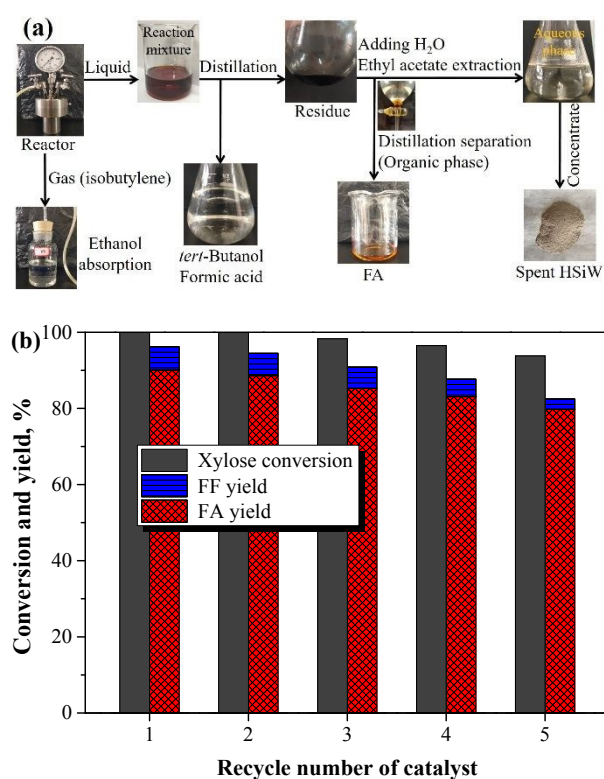


**Fig. 7.** The separation procedure of chemicals from reaction mixture (a), and reusability test of HSiW catalyst in the conversion of xylose to FA (b). Reaction conditions: 1 mmol xylose, 0.1 mmol HSiW, 27 mL *tert*-butanol, 3 mL formic acid, 130 °C, 3 h.

### Chemical separation and catalyst recycling

A graphic separation procedure of chemicals from the resulting reaction mixture is illustrated in Fig. 7a. After the reaction was quenched, gas products (mostly isobutylene) existing the reactor were primitively discharged by a special gas sampling system and collected by means of ethanol absorption. Quantitative analysis shows that isobutylene of *ca.* 26% yield was obtained from the acid-catalyzed intramolecular dehydration of *tert*-butanol. The released isobutylene, one of the most important lighter olefins, is mainly used in production of methyl methacrylate, butyl rubber and alkyl *tert*-butyl ethyl.<sup>33</sup> Then, the mixture solvent of *tert*-butanol and formic acid in the reaction solution was gathered by vacuum distillation at a low temperature of 60 °C, which can be recycled in the succeeding runs. Afterwards, H<sub>2</sub>O was added to the remaining liquid layer, and it was washed three times with ethyl acetate to extract the products and leave the catalyst in the aqueous phase. The formed aqueous phase was condensed to obtain the spent HSiW with a recovery rate of *ca.* 95%. The ethyl acetate was separated from the collected organic phase under vacuum to leave the products. The isolated yield of FA was close to the direct-detected yield of FA in the reaction mixture by GC analysis.

The recycling experiments showed from Fig. 7b that the recovered HSiW remained catalytically active with a slight decline both in xylose conversion and product yields over five successive runs, indicating a good reusability. A little by little deactivation of HSiW in recycle runs could be attributable to the adsorption and interference of polymeric by-products on the recovered catalyst, which was roughly judged by

the catalyst color varying from white to gray after use. FTIR spectrum of the spent HSiW after five recycles revealed four characteristic vibration peaks of Keggin structure HSiW anion in 700–1100 cm<sup>-1</sup> (see Fig. S9a). In addition, the spent and fresh HSiW demonstrated similar XRD patterns, in which characteristic diffraction peaks of HSiW were observed at the four intervals of 2θ of 7–13°, 16–23°, 25–30° and 30–38° (see Fig. S9b), meaning the retention of Keggin-type heteropolyanionic structure. All the above results suggest that commercial HSiW is a recyclable and stable heterogeneous catalyst for one-pot conversion xylose to FA in *tert*-butanol/formic acid mixed solvent.

### Conclusions

The present study successfully developed a facile and efficient protocol for the production of FA from xylose over heteropolyacids in *tert*-butanol/formic acid co-solvent that allows the reaction to proceed in one-pot with an excellent yield and in the absence of external H<sub>2</sub>. The solvent *tert*-butanol played multiple roles as a precursor of hydrogen honor and as a shield to facilitate xylose dehydration and stabilize the resultant FA. Commercial H<sub>4</sub>SiW<sub>12</sub>O<sub>40</sub> served as a multifunctional catalyst during the cascade reaction. The Brønsted and Lewis acid sites co-existed cooperatively catalyze the xylose dehydration step, and the owned active metal site of W atom adsorbs hydrogen proton to transfer hydrogenation of furfural to FA. After the incorporation of formic acid as a supplemental hydrogen source, an unprecedented FA yield of 90% was achieved in a batch reactor under mild conditions. The kinetic behavior describing the conversion of xylose into FA was determined to monitor the process. The chemoselective production of FA can be effectively regulated by the management of operating temperature. The catalyst, solvent and product could be separated from the reaction mixture, and the spent catalyst showed a good reusability. In conclusion, this proposed strategy has many advantages over those available towards the production of FA from xylose, such as straightforward manner, the nonuse of costly catalyst and molecular H<sub>2</sub>, high yield and being a green route.

### Experimental

#### Chemical reagent

Xylose, alkyl xyloside, furfural (FF), furfuryl alcohol (FA), and heteropolyacids including H<sub>4</sub>SiW<sub>12</sub>O<sub>40</sub> (HSiW), H<sub>3</sub>PW<sub>12</sub>O<sub>40</sub> (HPW) and H<sub>3</sub>PMo<sub>12</sub>O<sub>40</sub> (HPMo), were purchased from Aladdin Reagent (Shanghai, China). Methanol, ethanol, *n*-propanol *iso*-propanol, *n*-butanol, *sec*-butanol, *tert*-butanol, and formic acid were supplied by Sinopharm Chemical Reagent Co., Ltd. (Shanghai, China). All chemicals have been used as received.

#### Catalytic reaction procedure

All catalytic reactions were carried out in a 100 mL cylindrical stainless steel pressurized batch reactor equipped with an adjustable electric stove and magnetic stirrer. A typical procedure of the conversion of xylose into FA is described as follows: 1 mmol of xylose, 0.1 mmol of HSiW, and a 30 mL mixture solution composed of 27 mL *tert*-butanol and 3 mL formic acid were charged into the reactor. The

reactor was sealed, and then brought to the stated temperature by external heating and continuously stirred at 600 rpm for the reaction. After the designated reaction duration, the reactor was taken out and quickly placed into cold water to terminate the reaction. Gas products (mostly isobutylene) existing the reactor were firstly discharged by a special gas sampling system and collected to dissolve in a pure ethanol solution. Thereafter, the remaining sample take from the reactor was filtered with a 0.22  $\mu\text{m}$  syringe filter to obtain the liquid-phase products for further analysis. The procedure of other tests such as the effect of reaction system and process variables, as well as the reactivity of FF and FA, is similar to that of the above described.

### Product analysis

The products after the reaction were identified by an Agilent 7890 GC/5975 MS and a Shimadzu LC-10AVP HPLC analysis system. The qualitative analysis of FF and FA were determined by an Agilent 7820 GC instrument equipped with a flame ionization detector and a HP-5 capillary column (30 m  $\times$  0.32 mm  $\times$  0.25  $\mu\text{m}$ ).  $\text{N}_2$  was used as a carrier gas with a flow rate of 1.0 mL  $\text{min}^{-1}$ , the oven temperature was programmed from 60  $^\circ\text{C}$  to 90  $^\circ\text{C}$  at a heating rate of 5  $^\circ\text{C}/\text{min}$  and then to 230  $^\circ\text{C}$  at a heating rate of 20  $^\circ\text{C}/\text{min}$ , and the detector temperature was set at 250  $^\circ\text{C}$ . The concentration of sugars in the reaction solution was quantified using HPLC equipped with a Copsil  $\text{NH}_2$  column (250 mm  $\times$  4.6 mm) and a Waters 410 refractive index detector. The mobile phase was a mixture solution of acetonitrile and water at the flow rate of 1.0 mL  $\text{min}^{-1}$ , and the column was kept at 30  $^\circ\text{C}$ . The amounts of detected substances were calculated according to the external standard curves constructed as their authentic standards. Substrate conversion was based on the molar ratio of the substrate converted to the substrate loaded in the feed. The yields of FA, FF and alkyl xyloside were defined as the molar ratio of the obtained FA/FF/alkyl xyloside to the substrate loaded in the feed.

### Characterization of heteropolyacids

The heteropolyacids were characterized by pyridine-adsorbed Fourier transform infrared spectroscopy (Py-FTIR),  $\text{NH}_3$  temperature programmed desorption ( $\text{NH}_3$ -TPD),  $\text{H}_2$  temperature programmed reduction ( $\text{H}_2$ -TPR), powder X-ray diffraction (XRD), and Fourier transform infrared spectroscopy (FTIR) techniques. Py-FTIR test was performed on a PE Frontier spectrometer in the wavenumber range of 1600–1400  $\text{cm}^{-1}$ . Before analysis, 20 mg of sample was pressed into a wafer and placed inside an infrared cell at 400  $^\circ\text{C}$  for 2 h in vacuum, and this infrared spectrum was used as background for the Py-FTIR analysis. Then, the sample was exposed to pyridine vapour (2000 Pa) at 40  $^\circ\text{C}$  for 1 h, followed by reevacuation at 250  $^\circ\text{C}$  for 1 h before measuring the IR spectra. Absorption bands related to Lewis (1455  $\text{cm}^{-1}$ ) and Brønsted (1540  $\text{cm}^{-1}$ ) acid sites were integrated to determine the acidity of samples.  $\text{NH}_3$ -TPD and  $\text{H}_2$ -TPR were measured by using a ChemStar instrument equipped with a thermal conductivity detector, and the areas under the peaks were integrated to estimate the amount of adsorbed gas in the samples. Prior to the measurement, 200 mg of sample was preheated under a He flow (20 mL/min) at 600  $^\circ\text{C}$  for 0.5 h to remove adsorbed species on the surface, and then cooled down to 50  $^\circ\text{C}$ . For  $\text{NH}_3$ -TPD test, the

sample was treated by adsorption of  $\text{NH}_3$  in 10%  $\text{NH}_3$  gas flow for 1 h. After flushed in a flow of He gas (20 mL/min) for 1 h to remove the physically adsorbed  $\text{NH}_3$ , the TPD data was recorded from 50 to 600  $^\circ\text{C}$  with a ramp of 15  $^\circ\text{C}/\text{min}$ . The  $\text{H}_2$ -TPR test was conducted under a flow of  $\text{H}_2/\text{Ar}$  mixture (10%  $\text{H}_2$ ) by increasing the temperature to 700  $^\circ\text{C}$  with a heating rate of 10  $^\circ\text{C}/\text{min}$ . XRD patterns were taken using a Bruker D8 Advanced X-ray diffractometer with a Cu  $\text{K}\alpha$  radiation source operated at 40 kV and 30 mA, and data were collected from 2 $\theta$  between 5 $^\circ$  and 60 $^\circ$  with a step of 0.01 $^\circ$ . FTIR spectra were carried out by a Bruker Vertex 70 spectrometer in the range of 400–4000  $\text{cm}^{-1}$ , using KBr pellets and resolution of 0.5  $\text{cm}^{-1}$ .

### Conflicts of interest

There are no conflicts to declare.

### Acknowledgements

This work was financially supported by the National Natural Science Foundation of China (21965018), and Yunan Ten Thousand Talents Plan Young & Elite Talents Project.

### Notes and references

- (a) P. Sudarsanam, E. Peeters, E. V. Makshina, V. I. Parvulescu and B. F. Sels, *Chem. Soc. Rev.*, 2019, **48**, 2366–2421; (b) L. T. Mika, E. Csefalvay and A. Nemeth, *Chemical reviews*, 2018, **118**, 505–613; (c) C. Chatterjee, F. Pong and A. Sen, *Green Chem.*, 2015, **17**, 40–71.
- (a) A. Ibn Yaich, U. Edlund and A. C. Albertsson, *Chem. Rev.*, 2017, **117**, 8177–8207; (b) S. Kwak and Y. S. Jin, *Microb. Cell. Fact.*, 2017, **16**, 82. (c) X. Hu, S. Jiang, L. Wu, S. Wang and C. Z. Li, *Chem. Commun.*, 2017, **53**, 2938–2941; (d) D. S. Naidu, S. P. Hlangothi and M. J. John, *Carbohydr. Polym.*, 2018, **179**, 28–41; (e) P. Ponchai, K. Adpakpang, S. Thongratkaew, K. Chaipojjana, S. Wannapaiboon, S. Siwaipram, K. Faungnawakij and S. Bureekaew, *Chem. Commun.*, 2020, doi.org/10.1039/D0CC03424J.
- B. Danon, G. Marcotullio and W. de Jong, *Green Chem.*, 2014, **16**, 39–54.
- (a) D. Liu, D. Zemlyanov, T. Wu, R. J. Lobo-Lapidus, J. A. Dumesic, J. T. Miller and C. L. Marshall, *J. Catal.*, 2013, **299**, 336–345; (b) X. Li, P. Jia and T. Wang, *ACS Catal.*, 2016, **6**, 7621–7640.
- J. Long, W. Zhao, H. Li and S. Yang, In *Biomass, Biofuels, Biochemicals*, Elsevier, 2020, pp. 299–322.
- (a) A. Gandini, *Polym. Chem.*, 2010, **1**, 245–251; (b) M. Paniagua, J. A. Melero, J. Iglesias, G. Morales, B. Hernández and C. López-Aguado, *Appl. Catal. A-Gen.*, 2017, **537**, 74–82; (c) M. Arnaiz, V. Nair, S. Mitra and J. Ajuria, *Electrochim. Acta*, 2019, **304**, 437–446; (d) S. Deo, W. Medlin, E. Nikolla and M. J. Janik, *J. Catal.*, 2019, **377**, 28–40; (e) S. P. Verevkin, R. Siewert, and A. A. Pimerzin, *Fuel*, 2020, **266**, 117067.
- (a) R. Mariscal, P. Maireles-Torres, M. Ojeda, I. Sádaba and M. L. Granados, *Energ. Environ. Sci.*, 2016, **9**, 1144–1189; (b) S. Peleteiro, S. Rivas, J. L. Alonso, V. Santos and J. C. Parajo, *Bioresour. Technol.*, 2016, **202**, 181–191; (c) Y. Luo, Z. Li, X. Li, X. Liu, J. Fan, J. H. Clark and C. Hu, *Catal. Today*, 2019, **319**, 14–24; (d) J. Köchermann, J. Schreiber and M. Klemm, *ACS Sustain. Chem. Eng.*, 2019, **7**, 12323–12330; (e) R. Wang, X. Liang, F. Shen, M. Qiu, J. Yang and X. Qi, *ACS Sustain. Chem. Eng.*, 2019, **8**, 1163–1170; (f) H. Tian, Y. Shao, L. Zhang, P. Jia, Z. Zhang, Q. Liu, S. Zhang, Q. Liu, Y. Wang and X. Hu, *J. Chem. Technol. Biot.*, 2020, **95**, 1400–1411.
- (a) Y. C. He, Y. Ding, C. L. Ma, J. H. Di, C. X. Jiang and A. Y. Li, *Green Chem.*, 2017, **19**, 3844–3850; (b) Y. C. He, C. X. Jiang, J. W. Jiang, J. H. Di, F. Liu, Y. Ding, Q. Qing and C. L. Ma, *Bioresour. Technol.*, 2017, **238**, 698–705; (c) X. X. Xue, C. L. Ma, J. H. Di, X. Y. Huo and Y. C. He,

- Bioresour. Technol.*, 2018, **268**, 292–299; (d) J. H. Di, C. L. Ma, J. H. Qian, X. L. Liao, B. Peng and Y. C. He, *Bioresour. Technol.*, 2018, **262**, 52–58.
- 9 R. F. Perez and M. A. Fraga, *Green Chem.*, 2014, **16**, 3942–3950.
- 10 (a) R. F. Perez, S. J. Canhaci, L. E. P. Borges and M. A. Fraga, *Catal. Today.*, 2017, **289**, 273–279; (b) S. J. Canhaci, R. F. Perez, L. E. P. Borges and M. A. Fraga, *Appl. Catal. B-Environ.*, 2017, **207**, 279–285.
- 11 T. Deng, G. Xu and Y. Fu, *Chinese J. Catal.*, 2020, **41**, 404–414.
- 12 J. L. Cui, J. J. Tan, X. J. Cui, Y. L. Zhu, T. S. Deng, G. Q. Ding and Y. W. Li, *ChemSusChem*, 2016, **9**, 1259–1262.
- 13 (a) P. N. Paulino, R. F. Perez, N. G. Figueiredo and M. A. Fraga, *Green Chem.*, 2017, **19**, 3759–3763; (b) R. F. Perez, E. M. Albuquerque, L. E. Borges, C. Hardacre and M. A. Fraga, *Catal. Sci. Technol.*, 2019, **9**, 5350–5358.
- 14 (a) E. Ahmad, M. I. Alam, K. K. Pant and M. A. Haider, *Green Chem.*, 2016, **18**, 4804–4823; (b) M. Wang, L. Peng, X. Gao, L. He and J. Zhang, *Sustain. Energ. Fuel.*, 2020, **4**, 1383–1395.
- 15 M. Grasemann and G. Laurenczy, *Energ. Environ. Sci.*, 2012, **5**, 8171–8181.
- 16 (a) C. K. P. Neeli, Y. M. Chung and W. S. Ahn, *ChemCatChem*, 2017, **9**, 4570–4579; (b) J. Du, J. Zhang, Y. Sun, W. Jia, Z. Si, H. Gao, X. Tang, X. Zeng, T. Lei, S. Liu and L. Lin, *J. Catal.*, 2018, **368**, 69–78.
- 17 M. Lopes, K. Dussan and J. J. Leahy, *Chem. Eng. J.*, 2017, **323**, 278–286.
- 18 (a) T. Kim, R. S. Assary, C. L. Marshall, D. J. Gosztola, L. A. Curtiss and P. C. Stair, *ChemCatChem*, 2011, **3**, 1451–1458; (b) T. Kim, R. S. Assary, H. Kim, C. L. Marshall, D. J. Gosztola, L. A. Curtiss and P. C. Stair, *Catal. Today*, 2013, **205**, 60–66; (c) X. Li, Z. Zhang, L. Zhang, H. Fan, X. Li, Q. Liu, S. Wang and X. Hun, *Fuel*, 2020, **265**, 116961.
- 19 (a) T. W. Walker, A. K. Chew, H. Li, B. Demir, Z. C. Zhang, G. W. Huber, R. C. Van Lehn and J. A. Dumesic, *Energ. Environ. Sci.*, 2018, **11**, 617–628; (b) X. Luo, Y. Li, N. K. Gupta, B. Sels, J. Ralph and L. Shuai, *Angew. Chem. Int. Edit.*, 2020, doi: 10.1002/anie.201914703; (c) Y. Sun, K. Sun, L. Zhang, S. Zhang, Q. Liu, Y. Wang, T. Wei, G. Gao and X. Hu, *Energ. Fuel.*, 2020, **34**, 3250–3261; (d) Q. Lin, S. Liao, L. Li, W. Li, F. Yue, F. Peng and J. Ren, *Green Chem.*, 2020, **22**, 532–539.
- 20 M. A. Mellmer, C. Sener, J. M. R. Gallo, J. S. Luterbacher, D. M. Alonso and J. A. Dumesic, *Angew. Chem. Int. Edit.*, 2014, **53**, 11872–11875.
- 21 (a) G. Tsilomelekis T. R. Josephson, V. Nikolakis and S. Caratzoulas, *ChemSusChem*, 2014, **7**, 117–126; (b) M. A. Mellmer, C. Sanpitakseree, B. Demir, P. Bai, K. Ma, M. Neurock and J. A. Dumesic, *Nat. Catal.*, 2018, **1**, 199–207.
- 22 L. Shuai, M. T. Amiri, Y. M. Questell-Santiago, F. Heroguel, Y. Li, H. Kim, R. Meilan, C. Chapple, J. Ralph, J. S. Luterbacher, *Science*, 2016, **354**, 329–333.
- 23 (a) G. Brieger and T. J. Nestruck, *Chem. Rev.*, 1974, **74**, 567–580; (b) K. R. Enslow and A. T. Bell, *Catal. Sci. Technol.*, 2015, **5**, 2839–2847; (c) L. Hu, J. Xu, S. Zhou, A. He, X. Tang, L. Lin, J. Xu, Y. Zhao, *ACS Catal.*, 2018, **8**, 2959–2980.
- 24 (a) J. F. Knifton, J. R. Sanderson and M. E. Stockton, *Catal. Lett.*, 2001, **73**, 55–57; (b) D. Yang, C. A. Gaggioli, D. Ray, M. Babucci, L. Gagliardi and B. C. Gates, *J. Am. Chem. Soc.*, 2020, **142**, 8044–8056.
- 25 (a) J. Yuan, S. S. Li, L. Yu, Y. M. Liu, Y. Cao, H. Y. He and K. N. Fan, *Energ. Environ. Sci.*, 2013, **6**, 3308–3313; (b) D. F. Morais, R. A. Boaventura, F. C. Moreira and V. J. Vilar, *Appl. Catal. B-Environ.*, 2019, **249**, 322–332; (c) M. L. Granados, J. Moreno, A. C. Alba-Rubio, J. Iglesias, D. M. Alonso and R. Mariscal, *Green Chem.*, 2020, **22**, 1859–1872.
- 26 (a) M. N. Timofeeva, *Appl. Catal. A-Gen.*, 2003, **256**, 19–35; (b) K. I. Shimizu, H. Furukawa, N. Kobayashi, Y. Itaya and A. Satsuma, *Green Chem.*, 2009, **11**, 1627–1632.
- 27 (a) A. S. Dias, M. Pillinger and A. A. Valente, *J. Catal.*, 2005, **229**, 414–423; (b) I. Agirrezabal-Telleria, A. Larreategui, J. Requies, M. B. Guemez and P. L. Arias, *Bioresour. Technol.*, 2011, **102**, 7478–7485; (c) E. Lam, E. Majid, A. C. Leung, J. H. Chong, K. A. Mahmoud and J. H. Luong, *ChemSusChem*, 2011, **4**, 535–541; (d) Y. Liu, C. Ma, C. Huang, Y. Fu and J. Chang, *Ind. Eng. Chem. Res.*, 2018, **57**, 16628–16634; (e) F. Delbecq, Y. Wang, A. Muralidhara, K. El Ouardi, G. Marlair and C. Len, *Front. Chem.*, 2018, **6**, 146.
- 28 (a) V. Choudhary, A. B. Pinar, S. I. Sandler, D. G. Vlachos and R. F. Lobo, *ACS Catal.*, 2011, **1**, 1724–1728; (b) V. Choudhary, S. I. Sandler and D. G. Vlachos, *ACS Catal.*, 2012, **2**, 2022–2028; (c) Y. Yang, C. W. Hu and M. M. Abu-Omar, *ChemSusChem*, 2012, **5**, 405–410; (d) N. K. Gupta, A. Fukuoka and K. Nakajima, *ACS Catal.*, 2017, **7**, 2430–2436.
- 29 (a) P. Panagiotopoulou, N. Martin and D. G. Vlachos, *ChemSusChem*, 2015, **8**, 2046–2054; (b) M. J. Gilkey, P. Panagiotopoulou, A. V. Mironenko, G. R. Jenness, D. G. Vlachos and B. Xu, *ACS Catal.*, 2015, **5**, 3988–3994; (c) M. J. Gilkey and B. Xu, *ACS Catal.*, 2016, **6**, 1420–1436.
- 30 (a) X. Hu, R. J. Westerhof, D. Dong, L. Wu and C. Z. Li, *ACS Sustain. Chem. Eng.*, 2014, **2**, 2562–2575; (b) Y. Shao, K. Sun, L. Zhang, Q. Xu, Z. Zhang, Q. Li, S. Zhang, Y. Wang, Q. Lin and X. Hu, *Green Chem.*, 2019, **21**, 6634–6645.
- 31 (a) B. Danon, G. Marcotullio and W. de Jong, *Green Chem.*, 2014, **16**, 39–54; (b) V. Krzelj, J. Ferreira Liberal, M. Papaioannou, J. Van Der Schaaf and M. F. Neira d'Angelo, *Ind. Eng. Chem. Res.*, 2020, **59**, 11991–12003.
- 32 (a) P. D. Vaidya and V. V. Mahajani, *Ind. Eng. Chem. Res.*, 2003, **42**, 3881–3885; (b) S. Srivastava, N. Solanki, P. Mohanty, K. A. Shah, J. K. Parikh and A. K. Dalai, *Catal. Lett.*, 2015, **145**, 816–823.
- 33 (a) S. V. Kostjuk, *RSC Adv.*, 2015, **5**, 13125–13144; (b) D. I. Shiman, I. V. Vasilenko and S. V. Kostjuk, *Polym. Chem.*, 2019, **10**, 5998–6002; (c) T. Rajasekhar, G. Singh, G. S. Kapur and S. S. Ramakumar, *RSC Adv.*, 2020, **10**, 18180–18191.

## Table of Contents Entry

View Article Online  
DOI: 10.1039/D0GC02001J

### Graphic abstract:



### One sentence of text:

*tert*-Butanol protection enables chemoselective production of furfuryl alcohol directly from xylose over heteropolyacids using formic acid as a hydrogen donor.